9th International Modal Analysis Conference and Exhibit

LOCATION: FIRENZE INCONTRA, CENTRO AFFARI
FIRENZE (FLORENCE), ITALY

DATE: APRIL 14-18, 1991

REDUCED ORDER LINEAR MODELS OF A HYDRO-MECHANICAL MOUNT

Gun Kim
Research Associate

Raj Singh
Professor

Department of Mechanical Engineering
The Ohio State University,
Columbus, OH 43210-1107, USA

ABSTARCT

A detailed linear-time-invariant model with four degrees of freedom has been developed for a nonlinear hydro-mechanical mount to examine its characteristics and to understand the role of various components. The primary intent of this paper is to show that the reduced order dynamic models can describe the dynamic stiffness spectra adequately, but only at low frequencies. A good correlation between predictions and measured spectra has been found. The reduced order models can be used to study the vibration transmissibility and to carry out parametric design studies.

NOMENCLATURE

A_r	equivalent piston area of rubber
A_i	cross-sectional area of inertia track
b_r	damping coefficient of rubber
C_d	decoupler compliance
C	fluid compliance
f	frequency (Hz)
F	force
i	$\sqrt{-1}$
I_i	inertance of inertia track
k_r	spring constant of rubber
K	dynamic stiffness, F/x (ω)
l_i	inertia track length
m_E	engine mass
m_r	equivalent mass of rubber in shear mode
m_1, m_2	lumped fluid masses
p	pressure
q	flow rate
R	fluid resistance
s	Laplace transformation variable
t	time
x	displacement
x_a	amplitude of displacement
ϕ_K	loss angle or dynamic stiffness phase
ω	circular frequency (rad/s)
ω_n	natural frequency (rad/s)
ζ	damping ratio

SUPERSCRIPTS

-	static component of variable
t	total component of variable

1. INTRODUCTION

Hydro-mechnaical mounts, unlike conventional rubber mounts, can satisfy two essential but conflicting performance criteria for the automotive engine suspensions: (i) resonant motion control at lower frequencies and (ii) vibration isolation at higher frequencies [1-6]. However, this device is yet to be understood analytically. Accordingly a linear time-invariant (LTI) model is developed in this paper, even though such a device may be highly nonlinear. All of the hydro-mechanical mounts reported in the literature are conceptually similar but differ essentially in the design of the following: (i) inertia track which can be cylindrical [1] or spiral [2], and (ii) decoupler which can be a fixed [1] or free type [4]. Figure 1a shows a typical device with a free decoupler and cylindrical inertia track, and Fig.1b illustrates the device with a fixed decoupler.

2. MATHEMATICAL MODEL

A lumped parameter model is developed considering several control volumes as shown in Fig.1a [7,8]. For further details including assumptions involved, refer to our earlier paper [9]. One inertia lump has been chosen for each of the upper (#1) and lower (#2) chambers; see Nomenclature for the identification of symbols. The vehicle frame is assumed to be fixed. The excitation is applied by the engine through $F^t(t) = \bar{F} + F(t)$ or $x^t(t) = \bar{x} + x(t)$, where $\bar{F}$ is the engine weight or preload acting on rubber , $\bar{x}$ is the corresponding static displacement, and $F(t)$ and $x(t)$ are dynamic components. As shown in Fig.2a, the proposed lumped parameter model consists of six fluid control volumes, and three lumped masses m_1, m_2, and m_r. It has four dynamic degrees of freedom: $x^t(t)$, $x_1^t(t)$, $q_i^t(t)$, and $x_2^t(t)$. The governing equation of motion for rubber, from the Voigt model, is

$$F^t(t) - k_r x^t(t) - b_r \dot{x}^t(t) - A_r p_{11}^t(t) = m_r \ddot{x}^t(t) \qquad (1)$$

Application of the momentum balance to the fluid mass $m_1 = I_1 A_r^2$, control volumes #*i* and *d*, and fluid mass $m_2 = I_2 A_r^2$ of Fig.2a yields the following equations,

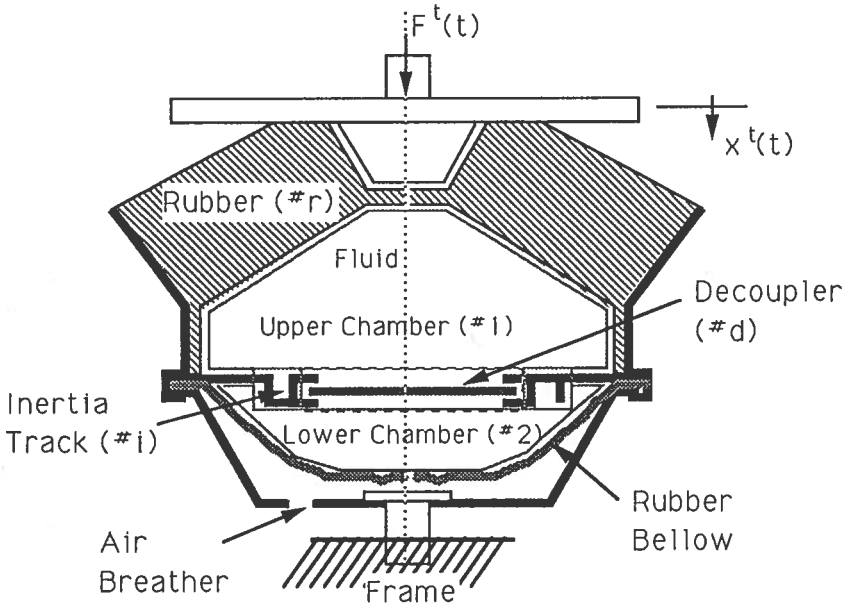

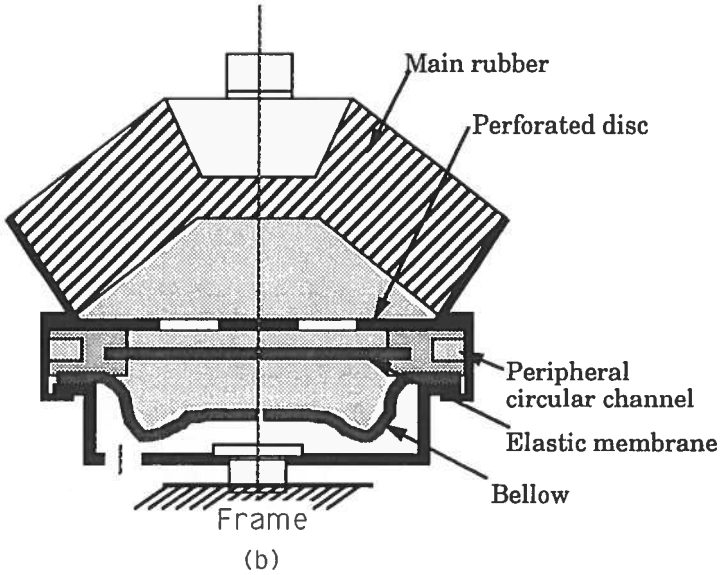

Figure 1. Hydro-mechanical mount example case.
(a) Physical system with a free decoupler, and lumping scheme.
(b) Physical system with a fixed decoupler.

$$\left[p'_{11}(t)-p'_{12}(t)\right]A_r = m_1\ddot{x}'_1(t) \tag{2}$$

$$p'_{12}(t)-p'_{21}(t) = R_d q'_d(t) = I_i\dot{q}'_i(t)+R_i q'_i(t) \tag{3}$$

$$\left[p'_{21}(t)-p'_{22}(t)\right]A_r = m_2\ddot{x}'_2(t) \tag{4}$$

Continuity equation applied to the compliant volume chambers of Fig.2a yields

$$A_r\left[\dot{x}'(t)-\dot{x}'_1(t)\right] = C_{11}\dot{p}'_{11}(t) \tag{5}$$

$$A_r\dot{x}'_1(t)-q'_d(t)-q'_i(t) = C_{12}\dot{p}'_{12}(t) \tag{6}$$

$$q'_d(t)+q'_i(t)-A_r\dot{x}'_2(t) = C_{21}\dot{p}'_{21}(t) \tag{7}$$

$$A_r\dot{x}'_2(t) = C_{22}\dot{p}'_{22}(t) \tag{8}$$

In the LTI analysis, C_{11}, C_{12}, C_{21} and C_{22} are assumed to be nominal time-invariant values. The static equilibrium value of each variable associated with the static load, given by a bar over the symbol, can be obtained from the following: $\overline{F} = F'(t)-F(t) = k_r\overline{x}+A_r\overline{p}_{11}$, $\overline{p}_{11}=\overline{p}_{12}=\overline{p}_{21}=\overline{p}_{22}=\overline{p}$, $\overline{q}_i=\overline{q}_d=0$, $A_r\overline{x} = A_r\left[x'(t)-x(t)\right] = \left[C_{11}+C_{12}+C_{21}+C_{22}\right]\overline{p}$, $A_r\overline{x}_1 = \left[C_{12}+C_{21}+C_{22}\right]\overline{p}$, $A_r\overline{x}_2 = C_{22}\overline{p}$. Eliminating the static components of the variables from Eqs.(1-8), identical equations will be obtained with only dynamic parts in terms of $F(t)$, $x(t)$, $p_{11}(t)$, etc. In Fig.2a, $F'_T(t)$ represents the transmitted force to the fixed frame which is measured typically in the experiment [10].

Consider the hydro-mechanical mount with a fixed decoupler where $q_i(t)$=0. Eliminating the internal variables $p_{11}(t)$, $p_{12}(t)$, $p_{21}(t)$, and $p_{22}(t)$ from Eqs.(1-8), and by defining $m_i = A_r^2 I_i$, $b_i = A_r^2 R_i$, $k_{11} = A_r^2/C_{11}$, $k_{12} = A_r^2/C_{12}$, $k_{21} = A_r^2/C_{21}$, $k_{22} = A_r^2/C_{22}$, and $\dot{x}_i(t) = q_i(t)/A_r$, we obtain the following four equations in terms of the time varying variables.

$$F(t)-k_{11}\left[x(t)-x_1(t)\right]-b_r\dot{x}(t)-k_r x(t) = m_r\ddot{x}(t)$$

$$k_{11}\left[x(t)-x_1(t)\right]-k_{12}\left[x_1(t)-x_i(t)\right] = m_1\ddot{x}_1(t)$$

$$-b_i\dot{x}_i(t)+k_{12}\left[x_1(t)-x_i(t)\right]-k_{21}\left[x_i(t)-x_2(t)\right] = m_i\ddot{x}_i(t)$$

$$k_{21}\left[x_i(t)-x_2(t)\right]-k_{22}x_2(t) = m_2\ddot{x}_2(t) \tag{9a-d}$$

From the above equations, an analogous mechanical system is developed in Fig.2b. This analog shows the operating principle of the hydro-mechanical mount. For a small $x(t)$, k_{12} become soft with the decoupler in the free travel mode. Namely, fluid damping b_i associated with the inertia track is decoupled from $x(t)$. Thus the engine is supported only by k_r and b_r. However, if $x(t)$ is large, k_{12} become stiff with the decoupler motion restrained by the snubbers. Namely b_i is coupled to $x(t)$. Thus the system is highly damped since $b_i >> b_r$. Observe that m_i is given by m_i multiplied by A_r^2, not by A_i^2. Since $m_i >> m_r$, and m_i is of the same order of magnitude as m_E, the inertia track performs as an inertia-augmented damping channel. Note that the analog mechanical system does not represent exactly the same dynamic system. For instance, the forces caused by $p'_{11}(t)$ and $p'_{12}(t)$ are directly transmitted to the vehicle frame from the hydro-mechanical mount, unlike the mechanical system of Fig.2b.

3. LOW FREQUENCY ANALYSIS

3.1. DEVELOPMENT OF MODEL II

Dynamics over the lower frequency range (1-50 Hz) are considered next. Since the impedances $i\omega I_1$ and $i\omega I_2$ of the lumped fluid masses are negligible at lower frequencies, a two-degree-of-freedom model can be developed as in Fig.3a. Here, $C_1 = C_{11}+C_{12}$, $C_2 = C_{21}+C_{22}$, $p_{11}(t) \approx p_{12}(t) = p_1(t)$, and $p_{21}(t) \approx p_{22}(t) = p_2(t)$. Using Eqs.(1-8), we get the following equations for a free decoupler in terms of the alternating components,

$$\begin{aligned} F(t)-k_r x(t)-b_r\dot{x}(t)-A_r p_1(t) &= m_r\ddot{x}(t)\\ p_1(t)-p_2(t) &= I_i(t)\dot{q}_i(t)+R_i q_i(t)\\ p_1(t)-p_2(t) &= R_d q_d(t)\\ A_r\dot{x}(t)-q_i(t)-q_d(t) &= C_1\dot{p}_1(t)\\ q_i(t)+q_d(t) &= C_2\dot{p}_2(t) \end{aligned} \tag{10a-e}$$

Eliminating the internal variables $p_1(t)$ and $p_2(t)$ from Eq.(10), and by defining $\dot{x}_i(t) = q_i(t)/A_r$, $m_i = A_r^2 I_i$, $b_i = A_r^2 R_i$, $k_1 = A_r^2/C_1$, and $k_2 = A_r^2/C_2$ for a device with a fixed decoupler, we obtain two governing equations corresponding to an analogous mechanical system of Fig.3b.

$$F(t)-b_r\dot{x}(t)-k_1\left[x(t)-x_i(t)\right]-k_r x(t) = m_r\ddot{x}(t)$$

$$-b_i\dot{x}_i(t)+k_1\left[x(t)-x_i(t)\right]-k_2 x_i(t) = m_i\ddot{x}_i(t) \tag{11a-b}$$

Equation (10) can be transformed to the Laplace domain with zero initial conditions to yield the following.

$$\frac{F}{x}(s) = \frac{\alpha_4 s^4+\alpha_3 s^3+\alpha_2 s^2+\alpha_1 s+\alpha_0}{\beta_2 s^2+\beta_1 s+\beta_0}$$

$$\alpha_4 = m_r C_1 C_2 R_d I_i,\ \alpha_3 = b_r C_1 C_2 R_d I_i + m_r C_1 C_2 R_d R_i + m_r I_i\left(C_1+C_2\right)$$

$$\begin{aligned} \alpha_2 &= m_r\left(R_i+R_d\right)\left(C_1+C_2\right)+b_r C_1 C_2 R_d R_i\\ &\quad + b_r I_i\left(C_1+C_2\right)+A_r^2 C_2 R_d I_i + k_r C_1 C_2 R_d I_i\\ \alpha_1 &= b_r\left(R_i+R_d\right)\left(C_1+C_2\right)+k_r C_1 C_2 R_d R_i\\ &\quad + k_r I_i\left(C_1+C_2\right)+A_r^2 I_i + A_r^2 C_2 R_d R_i\\ \alpha_0 &= k_r\left(R_d+R_i\right)\left(C_1+C_2\right)+A_r^2\left(R_d+R_i\right)\\ \beta_2 &= C_1 C_2 R_d I_i,\ \beta_1 = C_1 C_2 R_d R_i + I_i\left(C_1+C_2\right),\\ \beta_0 &= \left(R_d+R_i\right)\left(C_1+C_2\right) \end{aligned} \tag{12a-i}$$

The transmitted force and dynamic stiffness $K(s)$ are defined as

$$F_T(t) = k_r x(t)+b_r\dot{x}(t)+p_1(t)A_r \tag{13}$$

$$K(s) = \frac{F_T}{x}(s) = \frac{\hat{\alpha}_3 s^3+\hat{\alpha}_2 s^2+\alpha_1 s+\alpha_0}{\beta_2 s^2+\beta_1 s+\beta_0}, \tag{14}$$

where $\hat{\alpha}_2 = C_1 C_2 R_d\left(b_r R_i + k_r I_i\right)+b_r I_i\left(C_1+C_2\right)+A_r^2 C_2 R_d I_i$, and

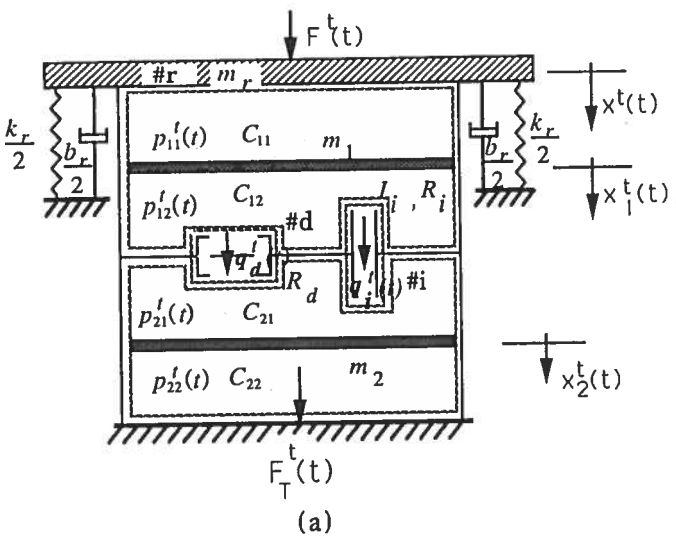

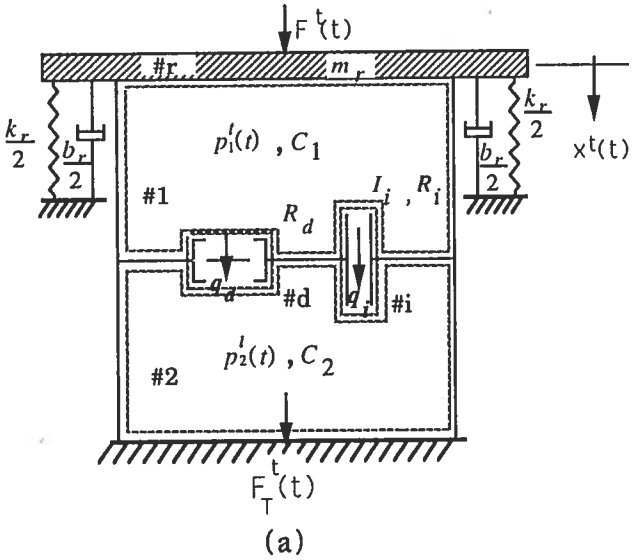

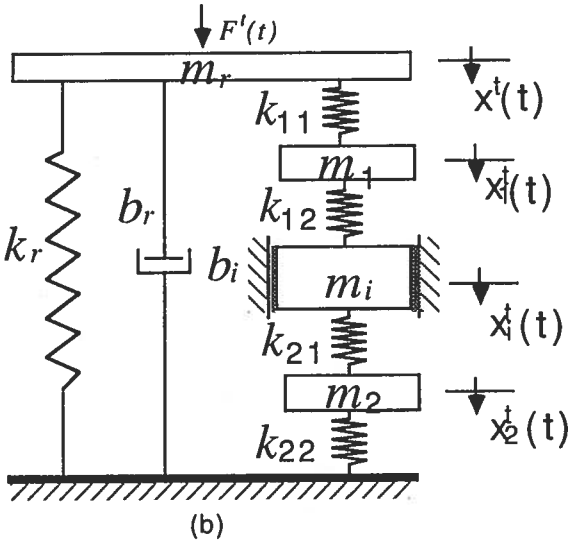

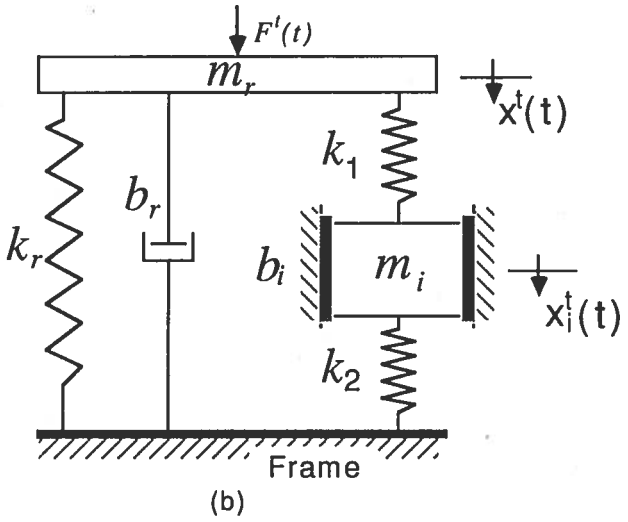

Figure 2. Mathematical model I.
(a) Schematic with a free decoupler.
(b) Analogous mechanical system with a fixed decoupler.

Figure 3. Mathematical model II.
(a) Schematic with a free decoupler.
(b) Analogous mechanical system with a fixed decoupler.

$\hat{\alpha}_3 = b_r C_1 C_2 R_d I_i$, while other parameters are given in Eq.(12). Observe that $K(s)$ is a system of (3rd order)/(2nd order). Sinusoidal dynamic stiffness $K(i\omega)$ is given by substituting $s=i\omega$ into Eq.(14).

$$K(i\omega) = |K(i\omega)|e^{i\phi_K(\omega)}$$
$$= |K(i\omega)|\cos\phi_K(\omega) + i|K(i\omega)|\sin\phi_K(\omega) \qquad (15)$$

3.2. REDUCED-ORDER FORM OF MODEL II

Since the influence of b_r over 1-50 Hz is negligible, assume that b_r=0. Noting further that $C_2 \geq 100C_1$, $K(s)$ can be simplified to a (2nd order)/(2nd order) system.

$$K(s) \approx \gamma \frac{\left(\frac{s^2}{\omega_{n1}^2} + \frac{2\zeta_1 s}{\omega_{n1}} + 1\right)}{\left(\frac{s^2}{\omega_{n2}^2} + \frac{2\zeta_2 s}{\omega_{n2}} + 1\right)} \qquad (16)$$

where $\gamma = k_r + \left[A_r^2/(C_1+C_2)\right]$ is the static stiffness. Other system parameters are given in Table 1 for both fixed and free decouplers. Here ζ is the damping ratio, and ω_n is the natural frequency. When we set $R_d \to \infty$ in the free decoupler expression, we obtain the results of the fixed decoupler since $R_d \to \infty$ corresponds to $q_d(t) \to 0$. Note that ω_{n2} of the fixed decoupler is equal to the natural frequency of a single degree of freedom Helmholtz resonator with compliance C_1 and inertance I_i.

The typical frequency response for both fixed and free decouplers with x_a=1.0mm is graphed in Fig.4 where $f=\omega/2\pi$, and the computed values of their system parameters are listed in Table 2. The difference in the frequency responses can be attributed to $q_d(t)$. It is seen from Table 2 and Fig.4 that $q_d(t)$ increases ζ_1 and ζ_2, and shifts ω_{n1} and ω_{n2} while decreasing $|K(i\omega)|$ and $\phi_K(\omega)$ for the free decoupler, compared to the fixed decoupler. Further research should investigate thoroughly the overall effect of $q_d(t)$ on the transmissibility of engine excitation to the chassis.

4. RESULTS

The Voigt model for rubber, and the proposed mathematical models I and II are verified by using the experimental results. The rubber mount case is realized by draining fluid from the hydro-mechanical mount. Since $k_r \neq k_r(\omega;x)$ and $b_r \neq b_r(\omega;x)$ for the Voigt model, $K(i\omega)=k_r+i\omega b_r$ in Fig.5, where b_r and k_r are the nominal values. The Voigt model represents the dynamic response of rubber reasonably well. The experimental results show that b_r and k_r vary with ω slightly. For instance, k_r=1.06k_{r0} at 50 Hz, and k_r=1.5k_{r0} at 250 Hz, where k_{r0} is the static spring constant. Thus the Voigt model for rubber is adequate in this LTI analysis.

Dynamic stiffness spectra as predicted by Models I and II, and by the reduced-order formulation of Eq.(16), are compared with measured results in Fig.6. We observe an excellent agreement even though the simulation is limited to a linear analysis. Further, the reduced-order formulation Eq.(16) shows a close agreement with the full-order formulation given by Eq.(14) and experiment. Thus, the hydro-mechanical mount can be represented as a (2nd order)/(2nd order) system for a high amplitude excitation over 1-50 Hz. This is due to the effect of third zero, say the third root of the numerator of Eq.(14) which is located around 1100 Hz, which is negligible over 1-50 Hz.

When x_a is reduced to 0.1mm, C_1 increases because the decoupler is essentially in the free travel mode. Corresponding spectra are graphed in Fig.7. It is seen that Model I or II predicts the experimental results reasonably well and that spectra are similar to those of the rubber mount shown in Fig.6. Hence, the hydro-mechanical mount behaves like the rubber mount for a low amplitude engine excitation at lower frequencies.

5. CONCLUDING REMARKS

Most, if not all, of the mathematical models available in the literature [1-5,9] can be shown to be the special cases of Model I or II. For instance, consider the viscoelastic model given by Corcoran and Ticks [2]. It is a simplified form of Model II where the fluid part is defined by a global spring stiffness and a viscous damping coefficient. Clark [3] also explains low frequency behavior analytically by using a mechanical model with a spring and damper. He represents $K(i\omega)$ as a (1st order)/(1st order) system. However, since the augmented inertial effect of the inertia track is significant, $K(i\omega)$ must be expressed at least as a (2nd order)/(2nd order) system as discussed earlier. Flower [4] proposes simplified fluid and mechanical analogs similar to Model II, but without any analytical study. Sugino and Abe [5] develop an analogous mechanical model without utilizing the concept of fluid parameters.

In our study, several LTI models of the hydro-mechanical mount with nominal time-invariant values for the lumped mechanical and fluid elements have been developed and validated over 1-50 Hz. However, a nonlinear model might be needed to explain the higher frequency dynamics. It will be the subject of a future paper.

ACKNOWLEDGEMENT

The authors would like to thank Teledyne Industries for supporting this study under its research assistance program.

REFERENCES

1. M BERNUCHON 1984 SAE Technical Paper Series 840259. A New Generation of Engine Mounts.
2. P. E. CORCORAN and G. H. TICKS 1984 SAE Technical Paper Series 840407. Hydraulic Engine Mount Characteristics.
3. M. CLARK 1985 SAE Technical Paper Series 851650. Hydraulic Engine Mount Isolation.
4. W. C. FLOWER 1985 SAE Technical Paper Series 850975. Understanding Hydraulic Mounts for Improved Vehicle Noise, Vibration and Ride Qualities.
5. M. SUGINO and E. ABE 1986 SAE Technical Paper Series 861412. Optimum Application for Hydroelastic Engine Mount.
6. P. L. GRAF, R. SHOURESHI, J. STARKEY, D. NOVOTNY and R. W. STEVENS 1988 SAE Technical Paper Series 880074. Active Frame Vibration Control for Automotive Vehicles with Hydraulic Engine Mounts.
7. R. SINGH 1989 Notes on ME675 Course: Design of Fluid Power Systems. Department of Mechanical Engineering: The Ohio State University.
8. E. O. DOEBELIN 1972 System Dynamics: Modeling and

Response. Columbus: Merrill.
9. R. SINGH, G. KIM and P. V. RAVINDRA 1990 Submitted to The Journal of Sound and Vibration. Hydro-Mechanical Mount for Automotive Engine, Part I: Linear Analysis.
10. CARL SCHENCK AG CORP. 1985 Software Instruction Manual for Schenck Hydropuls-System.

Table 1. System parameters of Eq.(16).

	Fixed decoupler ($R_d \to \infty$)	Free decoupler (finite R_d)
ω_{n1}	$\sqrt{\frac{k_r}{I_i\left(A_r^2 + k_r C_1\right)}}$	$\sqrt{\left(\frac{R_i + R_d}{R_d}\right)\frac{k_r}{I_i\left(A_r^2 + k_r C_1\right)}}$
ω_{n2}	$\sqrt{\frac{1}{C_1 I_i}}$	$\sqrt{\left(\frac{R_i + R_d}{R_d}\right)\frac{1}{C_1 I_i}}$
ζ_1	$\frac{1}{2}\sqrt{\frac{R_i^2\left(A_r^2 + C_1 k_r\right)}{k_r I_i}}$	$\frac{1}{2}\left[\sqrt{\frac{R_d R_i^2\left(A_r^2 + C_1 k_r\right)}{k_r I_i\left(R_d + R_i\right)}} + \sqrt{\frac{k_r I_i}{R_d\left(R_d + R_i\right)\left(A_r^2 + C_1 k_r\right)}}\right]$
ζ_2	$\frac{1}{2}\sqrt{\frac{C_1 R_i^2}{I_i}}$	$\frac{1}{2}\left[\sqrt{\left(\frac{R_d R_i^2}{R_d + R_i}\right)\frac{C_1}{I_i}} + \sqrt{\frac{1}{R_d\left(R_d + R_i\right)}\frac{I_i}{C_1}}\right]$

Table 2. System parameters predicted by Eq.(16).

Parameter	Fixed decoupler ($R_d \to \infty$)	Free decoupler (finite R_d)
$\omega_{n1}/2\pi$	6.0 Hz	7.1 Hz
$\omega_{n2}/2\pi$	11.3 Hz	13.3 Hz
ζ_1	0.66	0.69
ζ_2	0.35	0.54

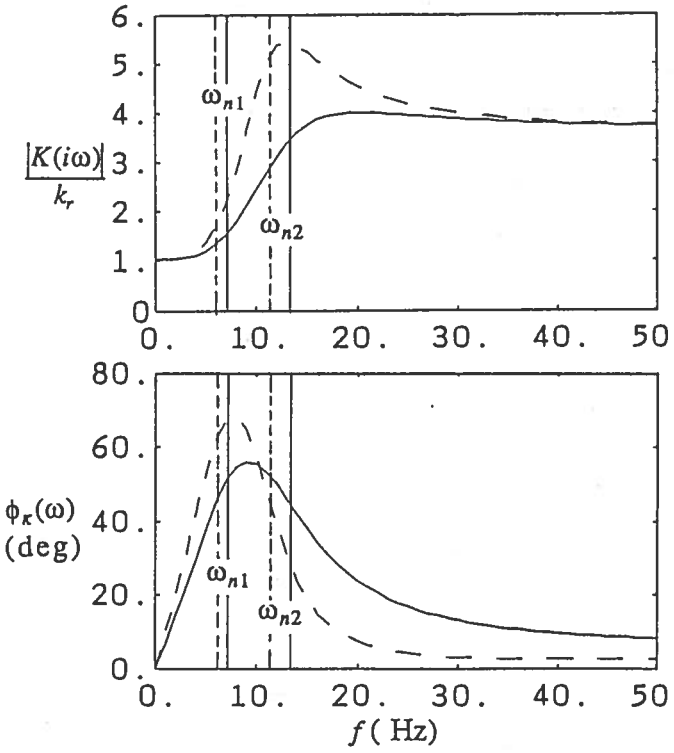

Figure 4. Frequency response predicted by Eq.(16) for fixed (– – –) and free (——) decouplers.

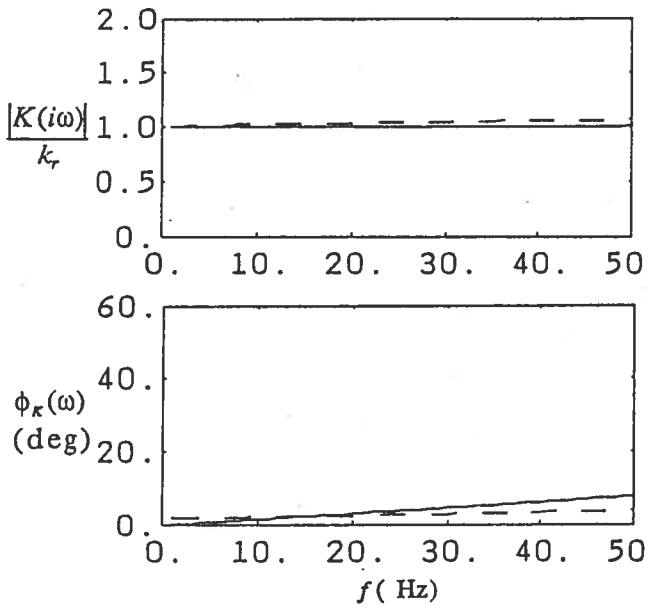

Figure 5. $K(i\omega)$ of rubber simulated by using a hydro-mechanical mount without fluid.
—— experiment, – – – Voigt model.

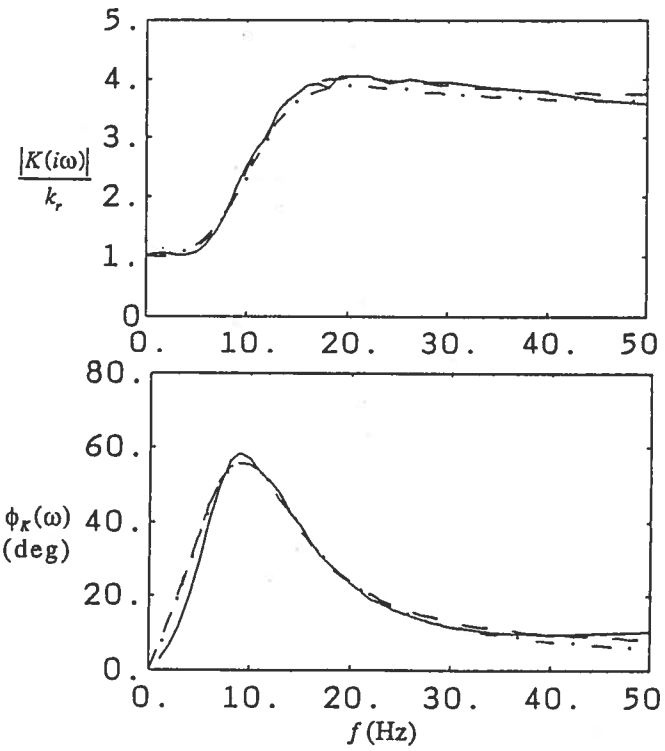

Figure 6. Dynamic stiffness with x_a=1.0mm.
—— experiment, – – – Models I and II,
– – – Eq.(16).

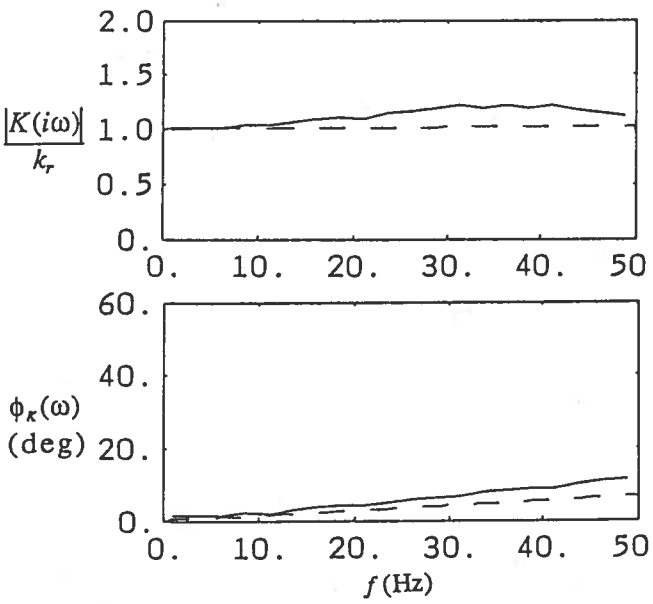

Figure 7. Dynamic stiffness with x_a=0.1mm.
—— experiment, – – – Model I and II.